The 9th European Congress on Computational Methods in Applied Sciences and Engineering
ECCOMAS Congress 2024
3 – 7 June 2024, Lisbon, Portugal

BUCKLING AND STRESS ANALYSIS FOR COMPOSITE PIPES UNDER THERMOMECHANICAL LOADING

OLEKSANDR MENSHYKOV[*], SUNNY O. UGUZO[*], MARINA MENSHYKOVA[*] AND MARIA KASHATALYAN[*]

[*] School of Engineering, University of Aberdeen, AB243UE Aberdeen, UK,
e-mail: o.menshykov@abdn.ac.uk, s.uguzo.21@abdn.ac.uk, m.menshykova@abdn.ac.uk,
m.kashtalyan@abdn.ac.uk, www.abdn.ac.uk

Key words: Finite Element Method, Buckling, Thermomechanical Loading, Composite Pipes.

Summary. The current study is focused on the buckling and stress analysis of multi-layered thermoplastic composite pipes under in-service loads corresponding to offshore deep-water operation scenarios considering changes in material properties due to the temperature gradient variation. The finite element model was developed and validated through the comparison with published analytical and numerical results. The effects of varying internal pipe and ambient seawater external pressure ratios and pipe geometry on buckling strength were assessed via finite element modelling, leading to viable engineering conclusions.

1 INTRODUCTION

The increased demand for deep water exploration of oil and gas products has necessitated the evolution of pipe materials from much heavier steel to fibre-reinforced polymers, which offer a range of advantages. These advantages include reduced weight, high specific strength and stiffness, etc. For composite pipes, instabilities like buckling or material failure inhibit load-bearing capability, deformation limits, structural integrity, and functionality. Hence, an appreciation of composite pipes' response to complex loading expected during in-service activities is essential for the optimal design of composite pipes.

Thus, numerous studies have been conducted to assess the feasibility of using composite pipes in the exploration of deep-water oil and gas resources encumbered by the environmental effects [1]. Emphasis has been placed on improving load-bearing capabilities, stability, and resistance to excessive deformation under various load spectrums. Effects of variations in geometry, ply number and thickness, ply orientation, stacking sequence, fibre and matrix volume fraction, and manufacturing techniques have also been explored.

The stresses and stress-strain response of thick-walled multi-layered composite pipes under bending were assessed in [2–4]. 3D analytical solutions were provided to study the through-thickness stress distribution changes due to varying fibre layer orientations. In [4] Tsai-Hill and maximum stress failure criteria were employed to evaluate the failure mechanism and flexural characteristics of a thermoplastic composite pipe (TCP) subjected to bending during spooling considering the material nonlinearities. In the study, factors affecting the optimal spool bend radius such as matrix strength and pipe wall buckling requirements were investigated using Finite Element Analysis (FEA).

Other studies have also evaluated the response of composite pipes under axial loading [5], pressure [6] and torsion [7]. In [5] the analytical model of helically armoured cable was adopted to identify the elastic-plastic behaviour of the HDPE material which predominantly opposed the axial load at less than 10% axial elongation. The changes in pipe tensile stiffness due to the fibre angle orientation increase were identified. In [6] the simplified elastic solution to appraise the stress state and deformation of multi-layered filament wound composite pipes under internal pressure was presented. A new approach for the pipe lay-up design introducing so called "safety zones" was suggested by Wang et al in [7]. Whereas, in [8] experiments and FEA were used predict the burst pressure of a TCP. A developed partially plastic theoretical model was also utilised to evaluate the uneven through-thickness stresses.

Studies have also considered the application of combined loads typically existent during pipe operational and installation activities. For instance, Bai et al [9] developed a theoretical model reliant on the natural catenary theory to assess the load distribution on a thick-walled TCP during J-lay offshore installation at 70m water depth subjected to bending and axial loads. The model was simplified by neglecting pipe bending stiffness. The failure and mechanical response of thick-walled TCP under simultaneous bending and pressure loading were analysed in [10] via FE modelling. The nonlinear characteristics of the pipe materials and failure mechanism along varying load paths were considered. A deterministic linear approach and a time step-based numerical algorithm for load application on the FE model were also employed.

Analysis of composite pipes subjected to combined axial, bending and pressure loads was also conducted by Gong et al [11]. The study appraised the buckling behaviour of composite pipes using FE simulation and a 2D analytical model which simplified the symmetry of buckling about the vertical plane and longitudinal evenness of deformity. The effect of varying D/t ranges and initial ellipticity were also considered.

Considering the operating environment and transportation of hydrocarbons, Xia et al [12] formulated an elastic solution based on the Classical Laminated Plate Theory to access the stress and deformation of a filament wound (FW) sandwich pipe under internal pressure and thermal loading. Similarly, in [13] a 3D anisotropic elasticity-based solution was presented to assess the thermal stresses and deformation of the multi-layered FW pipe subjected to internal pressure and thermal gradient. The study was focused on [+55/-55/+55/-55] and [+35/+35/90/90] ply stacking sequences due to their established low failure coefficients. Likewise, 3D FE models were used in [14, 15] to assess the through-thickness stresses and failure in multi-layered carbon fibre / PEEK TCPs subjected to pressure, axial and thermal loading of a single-leg hybrid riser system. The studies employed varying failure criteria to assess the influence of ply stacking sequence, load variation and geometry on the failure coefficients and stress distribution.

In the current study, the use of numerical modelling allowed to consider multiple load combinations. Furthermore, the dependence of composite material properties on temperature which has not been widely considered before due to sparse data can be necessarily achieved for more accurate stress, strain and failure predictions. Therefore, reflecting on current limitations on the application of composite pipes in deep water offshore oil and gas applications and increased drive to source resources at greater water depths, a 3D FEA study on thermoplastic composite pipes subjected to thermomechanical loading is presented here. Specifically, the influence of changing through-thickness thermal gradient on the buckling failure resistance is assessed.

2 PROBLEM STATEMENT

Operationally a typical TCP riser will be subjected to bending at the overhang and sag bend regions which can cause plastic deformation and ovality. Undulating seabed can also induce bending loads. Furthermore, pipes are subjected to external pressure due to water depths, which results in a combination of bending, pressure loads and axial loads. The introduction of pressurized fluids through the pipes generates internal pressure loads and through-thickness temperature gradients due to the movement of working fluids and the corresponding flow of seawater along the external surface of the pipe. A depiction of the sag bend region of a TCP riser which is the focus of this study, and the applied mechanical and thermal loads are shown in Figures 1 and 2.

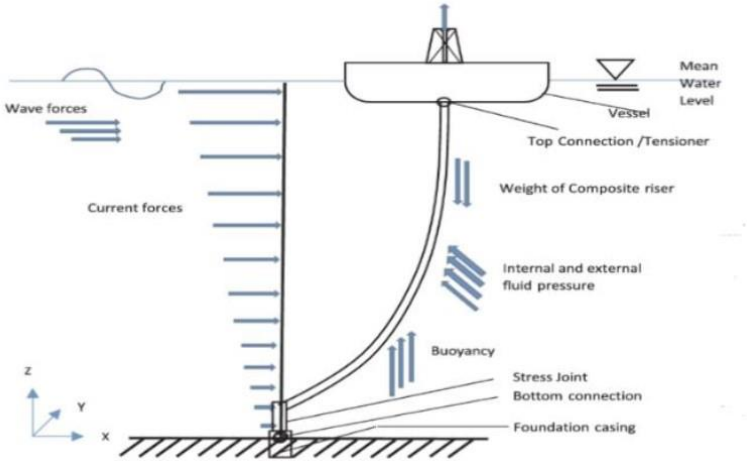

Figure 1: Standard installation and in-service loads [16].

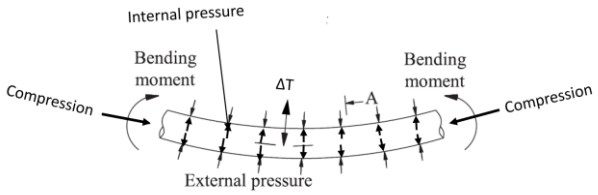

Figure 2: TCP riser under the loading

3. NUMERICAL MODELLING AND SIMULATION

3.1 Modelling methodology

Abaqus/CAE was utilised for numerical modelling in order to adequately simulate applied thermomechanical loads, boundary conditions and constraints. Solid elements were utilised due to the study's emphasis on thick-walled pipes. Additionally, the second-order hexahedral reduced integration elements C3D20R and C3D20RT were used for general static and couple temperature displacement analyses respectively.

Second-order elements were chosen to increase accuracy and reduce element distortion while using reduced integration resulted in reduced stiffness of the model and increased computational efficiency. Moreover, shear and volume lock were prevented. Mesh selection was based on findings from a mesh refinement study which was aimed to achieve an optimal blend of accuracy and computational efficiency.

3.2 Mechanical model validation

3.2.1 Combined pressure and axial loading

The model was validated for mechanical loads only and then for a combination of mechanical and thermal loads. The validation for mechanical loads was conducted in stages, where validation was firstly done for combined pressure and axial loads. Afterwards, the model was validated for bending and buckling (axial compression) loads. This method was adopted to ensure that the mechanical model was able to accurately predict stress distribution and deformation/displacement of the composite pipe under the prescribed loading spectrum.

The model configuration for validation of the model under combined pressure and axial loading was a TCP as adopted from Hastie et al [14]. The TCP configuration comprises homogenous APC-2 PEEK inner and outer liners and a unidirectional AS4/APC-2 carbon/PEEK reinforcement layer. Dimensions and loads applied on the TCP section are as detailed in Table 1. The material properties for the APC-2 PEEK and AS4/APC-2 carbon/PEEK are also stated in Tables 2 and 3 respectively. Through-thickness stresses comparison with existing model results are shown in Figure 3, which indicated a strong correlation

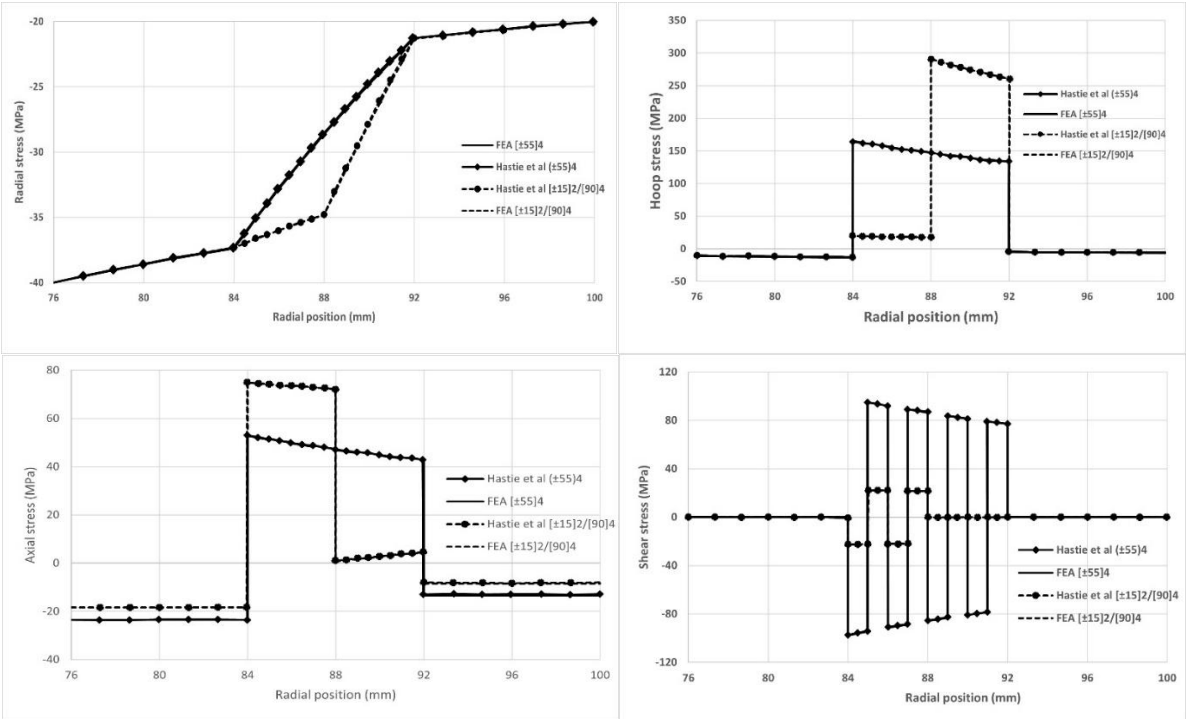

Figure 3: Radial (top left), hoop (top right), axial (bottom left), and shear (bottom right) stresses FEA validation for $[\pm 55]_4$ and $[\pm 15]_2$/ $[90]_4$ laminate ply orientations.

Table 1: TCP section basic configuration and applied loads (Hastie et al) [14].

Inner radius	Liner thickness	Cover thickness	External radius	Laminate thickness	Ply thickness	Axial load	Internal Pressure	Outside pressure
76 mm	8 mm	8 mm	100 mm	8 mm	1 mm	50 kN	40 MPa	20 MPa

Table 2: TCP material properties (Hastie et al) [14].

Property	E_1	$E_1 = E_2$	$G_{12} = G_{13}$	G_{23}	$v_{12} = v_{13}$	v_{23}
Unidirectional AS4/APC-2 carbon	142 GPa	9.6 GPa	6 GPA	3.6 GPa	0.37	0.33
APC-2 PEEK	4.1 GPa	-	-	-	0.41	-

3.2.2 Pure bending loading

Validation of pipe under pure bending load was done using a graphite/polymer multi-layered composite pipe adapted from Zhang et al [17]. Pipe material properties, geometry, ply angle orientation and applied load magnitude are shown in Tables 3 and 4. Through thickness stress distribution as shown in Figure 4 indicated good coincidence with the existing analytical solution [17].

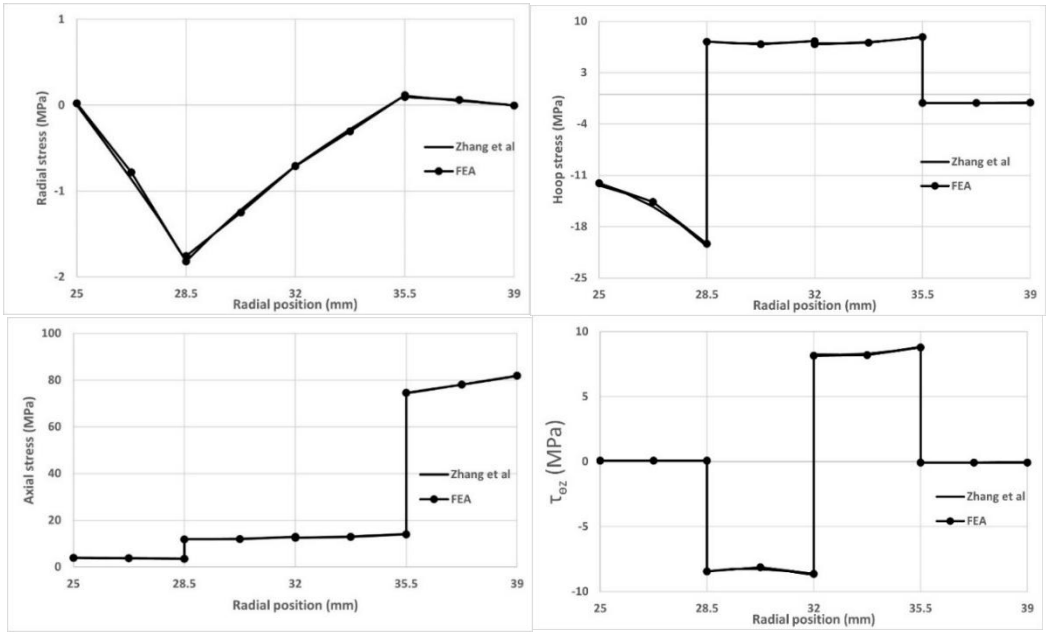

Figure 4: Composite pipe radial (top left), hoop (top right), axial (bottom left) and shear (bottom right) stress distribution comparison under bending load for ply angle [90/±45/0].

Table 3: Pipe geometry and ply angle orientation.

Properties	Inner radius	Outer radius	Laminae thickness	Laminate ply orientation	Pipe length	Applied moment
Value	25 mm	39 mm	3.5 mm	[90/±45/0]	500 mm	1.5101E6 Nmm

Table 4: Composite material engineering constants

E_{11}	$E_{22} = E_{33}$	G_{23}	$G_{13} = G_{12}$	v_{23}	$v_{13} = v_{12}$
155 GPa	12.1 GPa	3.2 GPa	4.4 GPa	0.458	0.248

3.2.3 Linear buckling load

Linear buckling analysis validation was conducted by subjecting a CFRP pipe to axial compression load as undertaken in [18]. The pipe's mechanical properties are given in Table 5. A critical buckling load of 239.2kN was obtained from the FEA conducted in comparison to the 240kN and 248.6kN loads obtained from the analytical and FEA outputs in the referenced literature. This represented percentage differences of 0.33% and 3.78% respectively. Similar buckling modes were also obtained (see Figure 5).

Table 5: Mechanical and geometric properties of the CFRP [18].

E_{11} (MPa)	E_{22} (MPa)	G_{12} (MPa)	v_{12}	Density (kg/m^3)	Thickness (mm)	Ply orientation
52,000	52,000	2350	0.302	1320	0.33	0/45/-45/0

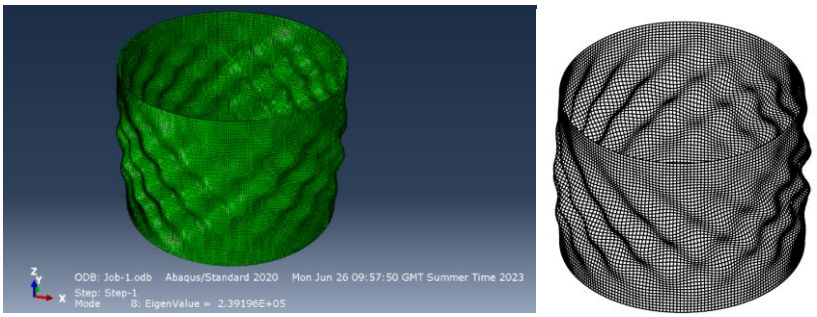

Figure 5: CFRP pipe buckling mode comparison for developed FEM (left) and reference model [18] (right).

3.2.4 Combined mechanical and thermal loads

The model in section 3.2.1 was modified to accommodate thermal loads. Temperature-dependent material properties of the TCP as obtained from published studies in [14, 15, 19–21] were implemented. Additionally, a coupled temperature-displacement step was utilised alongside an appropriate thermal solid element (C3D20RT). Increasing temperatures were applied as fixed boundary conditions in the internal surface of the TCP to represent varying fluid temperatures. On the external surface, a film coefficient was applied as a surface film condition to represent free convention to the surrounding sea environment.

Accordingly, FEA simulations were done for the TCP under internal pressure, external pressure and axial tension of 40MPa, 20MPa and 50kN respectively. TCP's internal surface temperature (T_i) was varied from 30–120^{o}C, while the film coefficient on the external surface incorporated a surrounding sea temperature of 4^{o}C and the heat transfer coefficient of 50Wm^{-2}C^{-1}. A predefined initial temperature of 23^{o}C was also defined for the TCP.

Through thickness temperature distribution for the TCP with $[\pm 55]_4$ reinforced layer configuration is shown in Figure 6, while the variation in stresses is shown in Figure 7.

A close correlation is noted between the FEA simulations and results obtained in [14]. The external pipe surface temperature for T_i = 30^{o}C and 120^{o}C were 8.9 ^{o}C and 27.1^{o}C, as recorded by Hastie et al [14], whilst the FEA simulation produced values of 8.93^{o}C and 27.8^{o}C with 0.33% and 2.6% differences respectively. This outcome validates the developed model for combined pressure, axial and thermal loads.

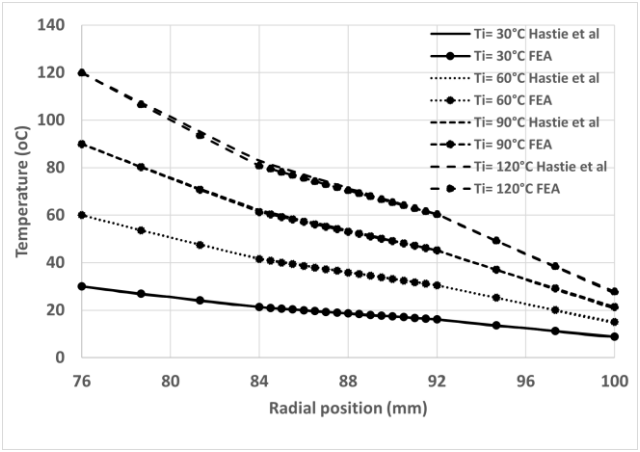

Figure 6: Through thickness temperature distribution comparison between FEA results and Hastie et al [14].

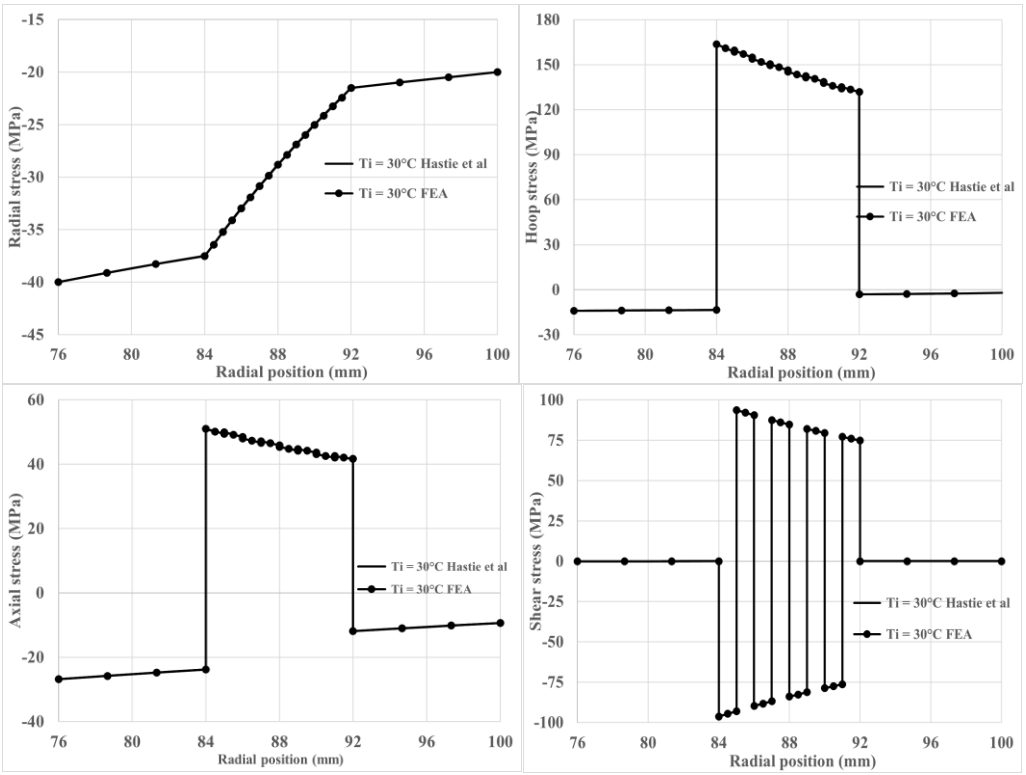

Figure 7: Stress variation comparison for $T_i = 30^oC$.

3.3 Linear buckling analysis under thermomechanical loading

3.3.1 Finite element model and applied loads

The linear bucking analysis under thermomechanical loading was conducted on a TCP adopted from Hastie et al [14] with similar geometry and properties as described in Tables 1 and 2. Additionally, a base pipe length of 3m was adopted. The selected pipe length concurred

with existing models [22, 23] where pipe lengths of 5D and 6.2D were recommended to accurately replicate the stress state and deformation mechanisms of a longer prototype. The recommended pipe length would also avoid end effects on the buckling or instability behaviour.

Uniform bending moment (M) and pressures (P_i and P_e) were applied along the pipe length in the first step of the analysis. Thermal loads arising from differences in temperature between the internal and external pipe surfaces were also implemented in the first step and propagated into the subsequent step. In the second step of the analysis, a compression load factor (F) of 1N was applied which evaluated the critical buckling load of the pipe from the preloaded state. Applied loads are described in section 3.2.4 alongside an assumed uniform bending moment of 1.5kNm. Kinematic coupling was employed to constrain pipe ends to centrally placed reference points, whilst meshing was achieved with C3D20RT elements.

3.3.2 Effect of changes in thermal gradient

The effect of increasing internal surface temperatures T_i on the critical buckling load (P_{cr}) corresponding to increasing through-thickness temperature gradient was analysed. The variation of P_{cr} with changing thermal gradient (load) is outlined in Table 6. A reduction of P_{cr} occurred as T_i was increased. In order words, as the thermal gradient was increased for the base pipe configuration and applied loads, P_{cr} decreased.

Table 6: Variation of critical buckling load with changes in pipe internal surface temperature.

Internal surface temperature	Critical linear buckling load, kN
4^{o}C (no thermal load)	1586.23
30^{o}C	1563.70
60^{o}C	1467.58
90^{o}C	1367.65
120^{o}C	1258.50

3.3.2 Effect of pressure load ratio variations

The effect of increasing T_i on the P_{cr} was analysed at varying internal to external pressure ratios for the TCP with a ply angle configuration of $[\pm 55]_4$. External pressures of 15 MPa, 20 MPa, 25 MPa and 30 MPa, corresponding to approximately 1500m, 2000m, 2500m and 3000m water depths were analysed. The P_i was varied for P_i/P_e = 1, 2 and 3. Internal surface temperature (T_i) was varied from 30^{o}C to 120^{o}C consistent with low and high thermal gradients. Constant sea temperature of 4^{o}C and the heat transfer coefficient of 50 $Wm^{-2}\ ^oC^{-1}$ were also implemented.

Figures 8 and 9 showed that when P_e is kept constant, regardless of the ratio of P_i/P_e, increasing T_i, i.e. thermal gradient, resulted in a reduction in $P_{cr.}$ Additionally, at constant T_i, the rate of decrease of P_{cr} is heightened as P_e is increased. For instance, at T_i = 30^{o}C and P_e = 15 MPa, a 14.67% and 17.19% decrease in P_{cr} was recorded as the P_i/P_e ratio varied from 1-2 and 2-3 respectively. However, at T_i = 30^{o}C and P_e = 20 MPa, 18.89% and 23.29% reduction in P_{cr} was noted as P_i/P_e ratio varied from 1-2 and 2-3. This heightened reduction rate of P_{cr} with increasing pressure was similar for varying values of $T_{i.}$ Furthermore, at constant low and high T_i (thermal gradient), P_{cr} increased with increasing P_e when P_i/P_e = 1. However, this trend is reversed for P_i/P_e = 2 and P_i/P_e = 3.

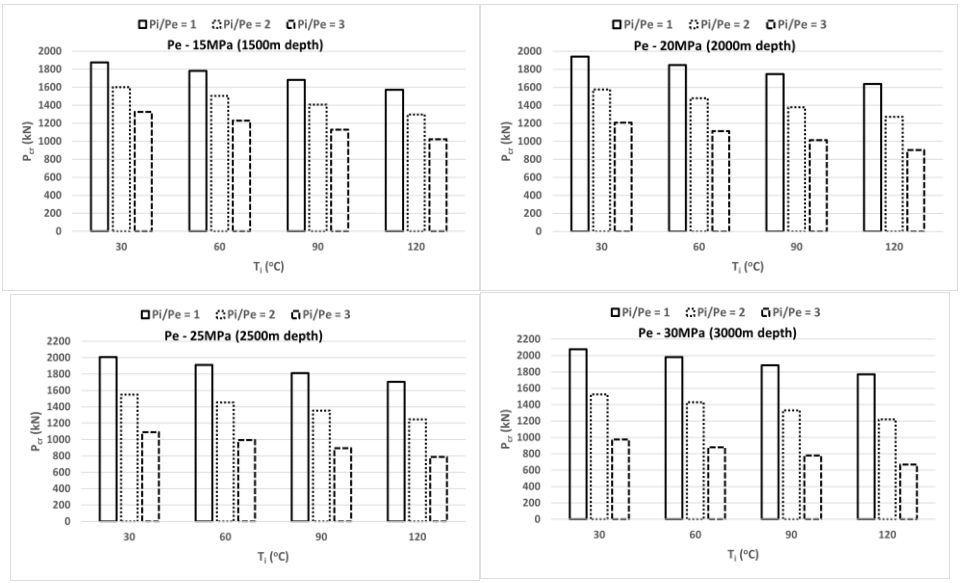

Figure 8: Effect of T_i on P_{cr} for different ratios of P_i/P_e.

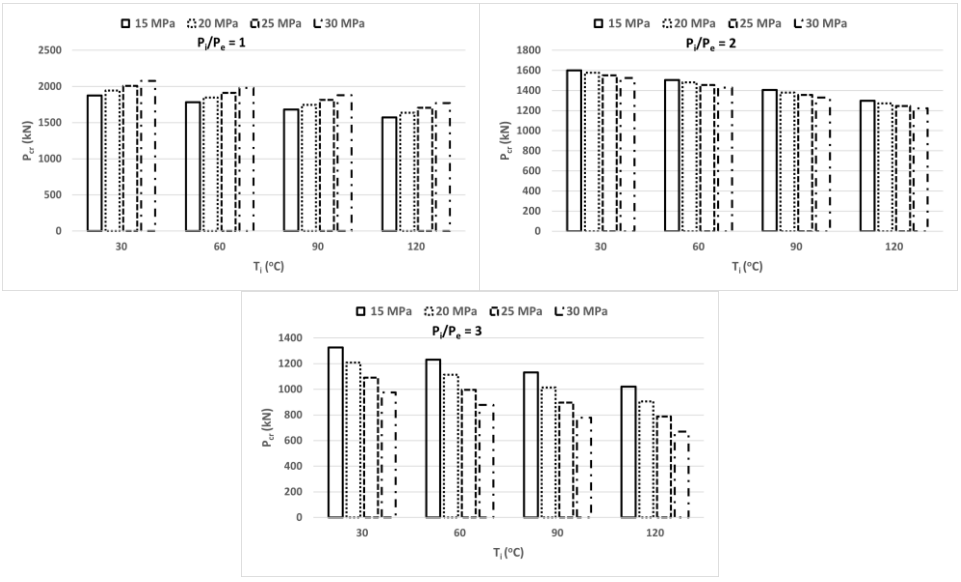

Figure 9: Effect of T_i on P_{cr} at varying water depths/external pressure values.

3.3.3 Effect of liner and cover thickness variations

The influence of changing the liner and cover thicknesses on the P_{cr} of the TCP was investigated. The base TCP configuration with equal liner, laminate and cover thicknesses of 8mm (8:8:8) was varied to 4:8:4, 12:8:12, 12:8:4 and 4:8:12 as depicted in Figure 10.

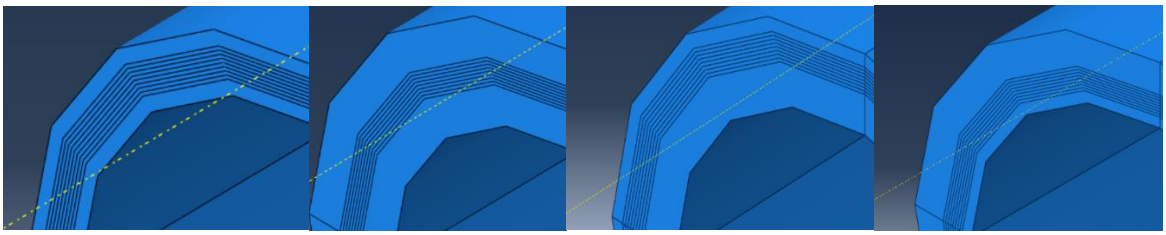

Figure 10: Pipe configuration for different ratios of liner/laminate/cover thicknesses

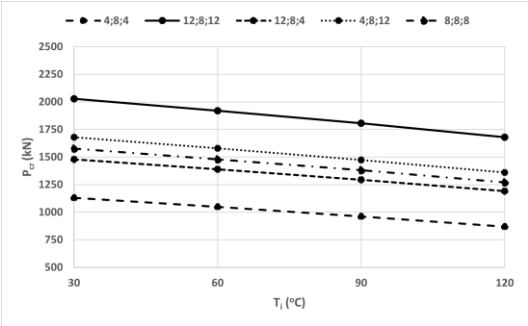

Figure 11: Critical buckling load vs. internal temperature for different ratios of liner/cover thickness.

Figure 11 indicates a reduction in P_{cr} with increasing T_i and thermal gradient for all liner/cover thickness configurations. Additionally, increasing the thickness of the liner and cover uniformly also increased the buckling strength of the pipe regardless of T_i or thermal gradient and vice versa. However, having a thicker inner liner and thinner cover affords the TCP less buckling strength when compared to the contrasting thickness configuration.

4. CONCLUSIONS

The buckling analysis of a TCP subjected to pressure, bending, axial and thermal loads was conducted via FE numerical modelling. Temperature-dependent engineering material properties were taken into consideration. The mechanical model employed was validated by comparing it with existing published results which showed good coincidence. A reduction in P_{cr} was witnessed when T_i was increased. Furthermore, increasing P_e enhanced the reductive influence of a higher thermal gradient on the P_{cr} of the TCP. However, at any value of T_i i.e. thermal gradient, P_{cr} increased as P_e was increased when $P_i/P_e = 1$. This trend reversed as the value of $P_i/P_e > 1$. It was also found that a uniform increase in liner and cover thickness yielded higher buckling strength and vice versa irrespective of T_i. However, increasing the outer cover thickness and reducing liner thickness improves buckling strength more than the alternative. Results obtained would be beneficial to assess the interactive correlation between buckling and material failure of the TCP under mechanical and thermal loads and the influence of changes in geometric and load factors.

REFERENCES

[1] Kyriakides, S., and E. Corona. 2007. *Mechanics of Offshore Pipelines: Buckling and Collapse*, First Edition, Vol. I.

[2] Xia, M., H. Takayanagi, and K. Kemmochi. 2002. "Bending behaviour of filament-wound fiber-reinforced sandwich pipes." Compos Struct 56(2): 201–210. https://doi.org/10.1016/S0263-8223(01)00181-7

[3] Wang, T., O. Menshykov, and M. Menshykova. 2024. "Novel computational model for the failure analysis of composite pipes under bending." Compos Sci Technol 256: 110757. https://doi.org/10.1016/j.compscitech.2024.110757

[4] Ashraf, M.A., E. V. Morozov, and K. Shankar. 2014. "Flexure analysis of spoolable reinforced thermoplastic pipes for offshore oil and gas applications," J Reinf Plast Compos 33(6): 533–542. https://doi.org/10.1177/0731684413491442

[5] Xu, Y., S. Lin, F. Pan, and Y. Bai. 2017. "Analysis of fibre glass pipe subjected to tensile load." in *Proceedings of the 27th International Ocean and Polar Engineering Conference*, ISOPE, 236–241.

[6] Xia, M., H. Takayanagi, and K. Kemmochi. 2001. "Analysis of multi-layered filament-wound composite pipes under internal pressure." Compos Struct 53(4): 483–491. https://doi.org/10.1016/S0263-8223(01)00061-7

[7] Wang, T., M. Menshykova, O. Menshykov, I.A. Guz, and N.K. Bokedal. 2023. "Mechanical analysis of thick-walled filament wound composite pipes under pure torsion load: safety zones and optimal design." Appl Compos Mater 30: 485–505. https://doi.org/10.1007/s10443-022-10088-3

[8] Shi, C., H. Xia, J. Wang, X. Bao, H. Li, and G. Fu. 2022. "Partially-plastic theoretical model of thermoplastic composite pipes and comparison of composite failure criteria." Compos Struct 280: 114834. https://doi.org/10.1016/j.compstruct.2021.114834

[9] Bai, Y., B. Yu, and P. Cheng. 2012. "Offshore installation of reinforced thermoplastic pipe (RTP)." in *Proceedings of the 22nd International Offshore and Polar Engineering Conference*, ISOPE, 101–108.

[10] Yu, K., E.V. Morozov, M.A. Ashraf, and K. Shankar. 2015. "Numerical analysis of the mechanical behaviour of reinforced thermoplastic pipes under combined external pressure and bending." Compos Struct 131: 453–461. https://doi.org/10.1016/j.compstruct.2015.05.033

[11] Gong, S.F., L. Yuan, and W.L. Jin. 2011. "Buckling response of offshore pipelines under combined tension, bending, and external pressure." J Zhejiang Univ Sci A 12: 627–636. https://doi.org/10.1631/jzus.A1000489

[12] Xia, M., K. Kemmochi, and H. Takayanagi. 2001. "Analysis of filament-wound fiber-reinforced sandwich pipe under combined internal pressure and thermomechanical loading." Compos Struct 51: 273–283. https://doi.org/10.1016/S0263-8223(00)00137-9

[13] Bakaiyan, H., H. Hosseini, and E. Ameri. 2009. "Analysis of multi-layered filament-wound composite pipes under combined internal pressure and thermomechanical loading with thermal variations." Compos Struct 88(4): 532–541. https://doi.org/10.1016/S0263-8223(01)00061-7

[14] Hastie, J.C., I.A. Guz, and M. Kashtalyan. 2019. "Effects of thermal gradient on failure of a thermoplastic composite pipe (TCP) riser leg." Int J Press Vessel Pip 172: 90–99. https://doi.org/10.1016/j.ijpvp.2019.03.027

[15] Hastie, J.C., M. Kashtalyan, and I.A. Guz. 2019. "Failure analysis of thermoplastic composite pipe (TCP) under combined pressure, tension and thermal gradient for an offshore riser application." Int J Press Vessel Pip 178: 103998. https://doi.org/10.1016/j.ijpvp.2019.103998

[16] Amaechi, C.V., N. Gillett, A.C. Odijie, X. Hou, and J. Ye. 2019. "Composite risers for deep waters using a numerical modelling approach." Compos Struct 210: 486–499. https://doi.org/10.1016/j.compstruct.2018.11.057

[17] Zhang, C., S.V. Hoa, and P. Liu. 2014. "A method to analyze the pure bending of tubes of cylindrically anisotropic layers with arbitrary angles including 0° or 90°." Compos Struct 109(1): 57–67. https://doi.org/10.1016/j.compstruct.2013.10.038

[18] Bisagni, C. 2000. "Numerical analysis and experimental correlation of composite shell buckling and post-buckling." Compos B Eng 31(8): 655–667. https://doi.org/10.1016/S1359-8368(00)00031-7

[19] Hastie, J.C., I.A. Guz, and M. Kashtalyan. 2021. "Numerical modelling of spoolable thermoplastic composite pipe (TCP) under combined bending and thermal load." Ships Offshore Struct 17(9): 1975–1986. https://doi.org/10.1080/17445302.2021.1958534

[20] Hastie, J.C., M. Kashtalyan, and I.A. Guz. 2021. "Analysis of filament-wound sandwich pipe under combined internal pressure and thermal load considering restrained and closed ends." Int J Press Vessel Pip 191: 104350. https://doi.org/10.1016/j.ijpvp.2021.104350

[21] Hastie, J.C., I.A. Guz, and M. Kashtalyan. 2020. "Structural integrity of deepwater composite pipes under combined thermal and mechanical loading." Procedia Struct Integr 28: 850–863. https://doi.org/10.1016/j.prostr.2020.11.053

[22] Tu, S., and J. Shuai. 2020. "Numerical study on the buckling of pressurized pipe under eccentric axial compression." Thin-Walled Struct 147: 106542. https://doi.org/10.1016/j.tws.2019.106542

[23] Yuan, L., Z. Liu, and N. Chen. 2022. "On the buckling of mechanically lined pipes under combined tension and bending." Ocean Eng 262: 111991. https://doi.org/10.1016/j.oceaneng.2022.111991